First-principles calculation of the electric-field gradient in hcp metals

P. Blaha and K. Schwarz
Institut für Technische Elektrochemie, Technische Universität Wien, A-1060 Vienna, Austria

P. H. Dederichs
Institut für Festkörperforschung, Kernforschungsanlage Jülich, D-5170 Jülich, Federal Republic of Germany
(Received 15 September 1987)

The electric-field gradient (EFG) for all hcp metals from Be to Cd is obtained from energy-band calculations using the full-potential linearized-augmented-plane-wave (LAPW) method. Our first-principles method, which does not rely on any Sternheimer antishielding factor, yields EFG's in good agreement with experiment and predicts also the sign of the EFG's. The EFG was found to be determined mainly by the nonspherical distribution of the valence-electron density close to the nucleus. In general, contributions to the EFG originating from p states dominate. This is the case even for transition metals, where the d anisotropy is large.

I. INTRODUCTION

All nuclei with a nuclear-spin quantum number $I \geq 1$ have a nonspherical nuclear charge distribution and an electric quadrupole moment Q. The interaction between this quadrupole moment Q and the electric field gradient (EFG) at the atomic site with noncubic point symmetry can be measured by various methods[1,2] and is used for the characterization of surfaces, impurities, and vacancies.[3,4]

While experimental techniques are highly sophisticated, the theoretical understanding of the origin of the EFG is poor. The current status of the theory was summarized recently.[5] For transition metals no reliable calculations of EFG's are reported in the literature. Most of the previous work is based on non-self-consistent orthogonalized-plane-wave (OPW) or pseudopotential calculations, which are not state-of-the-art band-structure methods. Often a partitioning into an ionic and a valence EFG is made, and these quantities are modified by antishielding functions $\gamma(\mathbf{r})$, which can only be crudely estimated, or by Sternheimer antishielding factors γ_∞, whose application is only justified if the EFG is due to a slowly varying external field.

Recently, Blaha *et al.*[6] developed a new method of calculating EFG's based on full-potential linearized-augmented-plane-wave (LAPW) calculations and applied it to Li_3N, a superionic conductor. Li_3N has three independent EFG's and they were calculated from first principles by means of two different ways of solving Poisson's equation. Both schemes gave excellent results in comparison to experimental data. In order to check this method in metallic systems we performed self-consistent full-potential LAPW band-structure calculations for Be, Mg, Sc, Ti, Co, Zn, Y, Zr, Tc, Ru, and Cd in the hexagonal-closed-packed (hcp) structure at the experimental lattice parameters.

II. METHOD

In the LAPW method[7] the unit cell is divided into nonoverlapping spheres (with radii R_t) and in an interstitial region; in the former the wave functions are expressed in atomiclike functions and in the latter in plane waves. The charge density (and analogously the potential) inside the spheres is written as a linear combination of radial functions $\rho_{LM}(r)$ times symmetrized lattice harmonics $Y_{LM}(\hat{\mathbf{r}})$ and as a Fourier series in the interstitial region:

$$\rho(\mathbf{r}) = \begin{cases} \sum_{L,M} \rho_{LM}(r) Y_{LM}(\hat{\mathbf{r}}) & \text{(inside sphere)} \\ \sum_{\mathbf{K}} \rho(\mathbf{K}) \exp(i\mathbf{K}\cdot\mathbf{r}) & \text{(interstitial)} . \end{cases} \quad (1)$$

Poisson's equation is solved according to a method proposed by Weinert.[8]

Since we calculate a full potential without any restrictions on its shape from the total charge density of the infinite system (including the nuclear charges), we can obtain the EFG V_{zz} directly from the $L=2$, $M=0$ component of the potential expansion inside the spheres:

$$V_{zz} = \left[\frac{5}{4\pi}\right]^{1/2} \lim_{r\to 0}[V_{20}(r)/r^2] , \quad (2)$$

and hence do not rely on additional Sternheimer factors or other (arbitrary) corrections. In Eq. (2) we assume that the main axis of the EFG tensor points in the z direction.

The solution of the boundary value problem[8] yields the radial potential coefficients $V_{LM}(r)$; thus the $L=2$, $M=0$ value at $r=0$ is directly available:

$$V_{20}(r=0)=\frac{4\pi}{5}\int_0^{R_t}\frac{\rho_{20}}{r^3}r^2dr$$

$$-\frac{4\pi}{5}\int_0^{R_t}\frac{\rho_{20}}{r^3}\left[\frac{r}{R_t}\right]^5 r^2dr$$

$$+4\pi\sum_{\mathbf{K}}V(\mathbf{K})\gamma_2(KR_t)Y_{20}(\hat{\mathbf{K}})\ . \tag{3}$$

The first term in the calculation of $V_{20}(0)$ corresponds to the well-known integral over the charge density times the $L=2$ Legendre polynomial divided by r^3, but integrated only over the atomic sphere. The second and third contributions arise from the charge density outside the considered sphere. The second term comes from solving the boundary value problem and guarantees that the potential matches at R_t.

The first part in Eq. (3) is named *valence EFG*, since it originates from the nonspherical electron density of the valence (and semicore) electrons within the atomic sphere. The sum of the second and third terms in Eq. (3) represents the *lattice EFG*, since they include a multipole summation. Note, that this splitting into two parts is formally exact (but depends on the choice of sphere radii) and thus is not identical to the common "valence" and "lattice" parts, which are only approximations since they require nonoverlapping charges.

In our computation the EFG is affected by the following three aspects.

(a) Numerical limitations in our band-structure code. Especially the small EFG's in Be,[9] Mg, and Co are affected by a finite **k** mesh. We have consistently taken about 800 **k** points in the irreducible wedge of the first Brillouin zone, while all other computational details are the same as in the work on Be.[9]

(b) The treatment of the core electrons. We have partitioned the core into semicore states (i.e., 1*s* for Be; 1*s* and 2*s* for Mg; 3*s* and 3*p* in the 3*d* series; and 3*d*, 4*s*, and 4*p* in the 4*d* series), which are treated completely as band states in the full (nonspherical) potential and true core states, which are treated atomiclike in the self-consistent muffin-tin potential (thawed core approximation).

(c) Our theoretical EFG's are based on band-structure calculations using the local-density approximation[10] (LDA) for exchange and correlation. Since the electron density is the key quantity in this theory, the EFG is a direct and very sensitive test of the validity of the LDA. The most critical quantity for us is the symmetry splitting of *p* or *d* states in a crystal, since in the LDA the effective potential is local and state independent, and thus may lead to a charge density whose anisotropy is not correctly described. Problems in the theoretical description of anisotropies for 3*d* metals show up, for instance, in bcc vanadium, where the x-ray form-factor ratios of the paired reflections (330)-(411) and (422)-(600) are severely underestimated by theory in comparison to experiment.[1]

III. RESULTS AND INTERPRETATIONS OF THE EFG

In Table I we list the experimental values[12–14] and our theoretical results for the EFG's of all hcp metals up to Cd. Note, that because of uncertainties in the values of the nuclear quadrupole constant Q and due to influences of structure and temperature in the respective experiments, error bars of approximately 10–20% exist in many cases. In view of this uncertainty the agreement is excellent. For the first time *one* theory is able to reproduce the experimental values of the EFG's in *all* hcp metals. We can reproduce the sign of the EFG where it is measured (Co, Zn, Ru, Cd) and predict interesting changes in the sign (indicated by $-$) of the EFG in the series Be–Mg; Sc, Ti–Co; and Y, Zr–Tc, Ru. Our theoretical value for Ti (69×10^{13} esu/cm^3) is in much better agreement with a recent measurement[13] than with the previous accepted value[12] (56 versus 36×10^{13} esu/cm^3). Hopefully these theoretical predictions will stimulate additional measurements of the EFG's including the sign.

A reliable theory of physical properties must not only be able to calculate the respective quantities accurately, but should also explore the origin of these quantities and provide a deeper understanding. So far, it was by no means clear what the main contributions to the EFG are. Do they come from the point charges of the lattice, from core or valence electrons, from *p* or *d* states? In the following we address these questions.

Above we have given our definition of the valence and the lattice EFG. In Table II both of these contributions are listed. The valence EFG dominates and the lattice EFG contributes 10–15% at most (except for Be). Previously, the traditional equation,[1]

$$V_{zz}=(1-\gamma_\infty)V_{zz}^{\text{latt}}+(1-R)V_{zz}^{\text{local}} \tag{4}$$

(where R is small but $|\gamma_\infty|$ can be quite large) was used in many attempts to explain EFG's basically from V_{zz}^{latt} alone, e.g., with the "universal correlation."[15] When we compare this traditional view with our results, we arrive at a completely different understanding of the EFG.

The lattice contributions are small compared to the

TABLE I. Theoretical and experimental EFG's (Refs. 1 and 12–14) (in 10^{13} esu/cm^3) for hcp elements. The sign of the experimental values is unknown if not given explicitly. The ideal c/a ratio is 1.633.

Element	c/a	Expt.	Theory
$_4$Be	1.56	1.6	−1.4
$_{12}$Mg	1.62	1.8	+1.6
$_{21}$Sc	1.59	13	+32
$_{22}$Ti	1.59	54	+69
$_{27}$Co	1.62	−9.6	−6.2
$_{30}$Zn	1.86	+120	+125
$_{39}$Y	1.57		+93
$_{40}$Zr	1.59	123	+143
$_{43}$Tc	1.60	23	−49
$_{44}$Ru	1.59	−32	−41
$_{48}$Cd	1.89	+230	+254

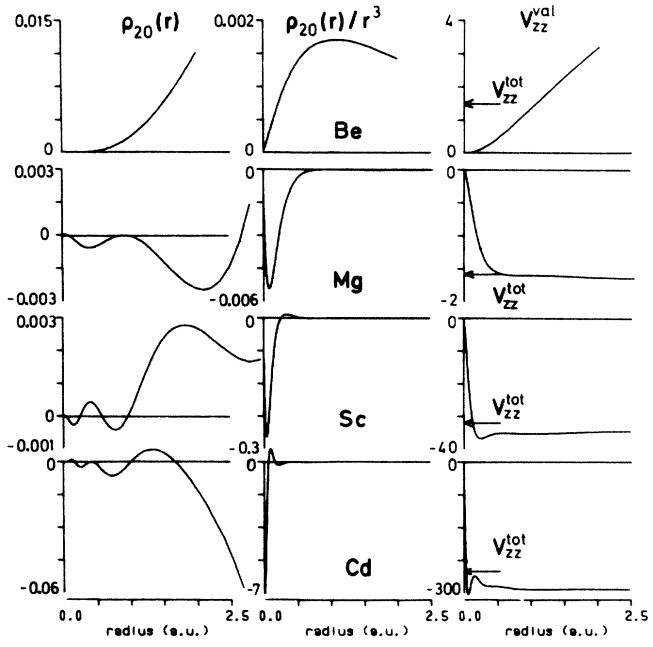

FIG. 1. Nonspherical charge-density component $\rho_{20}(r)$, the EFG integrand $\rho_{20}(r)/r^3$, and the valence EFG $V_{zz}^{val}(r)$ are plotted as a function of radius for Be, Mg, Sc, and Cd. The arrows indicate the total EFG.

direct local contributions. These local contributions to the EFG originate from the nonspherical charge density inside the atomic sphere. This charge density is built up from the core density (in our approximation always taken to be spherical), the semicore, and the valence contribution. The contribution from the semicore states (Table II) is found to be almost negligible, independent of the principle quantum number or the angular momentum of these states. Therefore we have neglected the "core polarization" of the deeper core states by forcing their charge density to be spherically symmetric.

The radial coefficient $\rho_{20}(r)$, which enters the integral in the EFG equation (3) can be obtained from the wave functions[7] by (in a short notation)

$$\rho_{20}(r)=\sum_{E_{nk}<E_F}\sum_{l,m}\sum_{l',m'}R_{lm}(r)R_{l'm'}(r)G_{2ll'}^{0mm'}\ , \qquad (5)$$

where R_{lm} denote the radial wave functions (of state E_{nk}) and $G_{Lll'}^{Mmm'}$ are Gaunt numbers, which vanish for most cases so that only a few terms remain in the double sum. For $L=2$, $M=0$ only p-p, d-d, and s-d combinations of l and l' are allowed. The $\rho_{20}(r)$ coefficients can be calculated separately for each combination, and the p-p and d-d contributions to the total EFG are given in Table II. (The mixed s-d term is negligible.) To our surprise we found that the EFG is dominated by p-p contributions not only in the sp metals, but also in the $3d$ and $4d$ transition-metal series, where the total p pop-

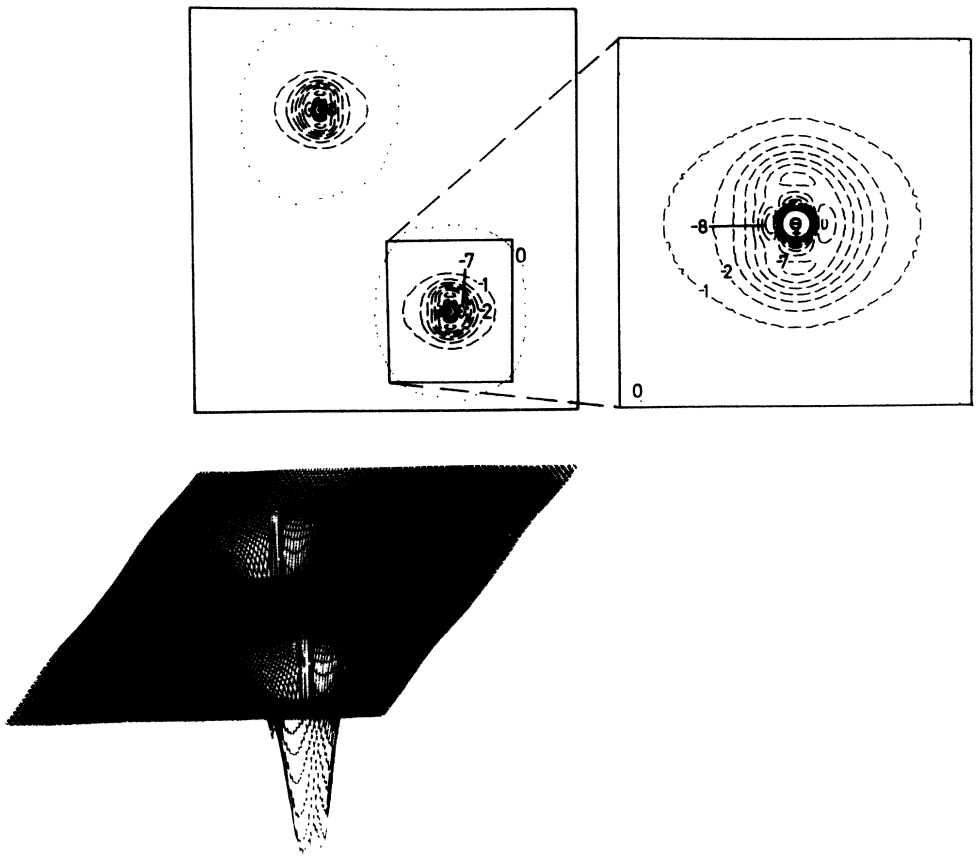

FIG. 2. Difference electron densities of hcp Zn in the $(11\bar{2}0)$ plane. The cutoff of the perspective plot is 0.08 e/a.u.^{3} In the contour plot units of me/a.u.^{3} are used.

TABLE II. Contributions to the total EFG V_{zz} from the "lattice" and "valence" parts (see text) and further decomposition of the "valence EFG" into *p-p*, *d-d*, and semicore contributions (in 10^{13} esu/cm^3) as well as the "nonspherical" *p* and *d* charges inside the muffin-tin sphere. [$\Delta n_p = 1/2(n_{p_x}+n_{p_y})-n_{p_z}$; $\Delta n_d = (n_{d_{xy}}+n_{d_{x^2-y^2}})-1/2(n_{d_{xz}}+n_{d_{yz}})-n_{d_{z^2}}$.]

Element	V_{zz}^{latt}	V_{zz}^{val}	$V_{zz}^{p\text{-}p}$	$V_{zz}^{d\text{-}d}$	V_{zz}^{semicore}	Δn_p	Δn_d
$_4$Be	+1.8	−3.2	−3.2	0	0	−0.010	
$_{12}$Mg	−0.1	+1.7	+1.7	0	0	+0.002	
$_{21}$Sc	−4	+36	+40	−5	+1	+0.015	−0.025
$_{22}$Ti	−14	+83	+48	+33	+2	+0.011	+0.086
$_{27}$Co	+1	−7	−13	+4	+2	−0.002	+0.003
$_{30}$Zn	−19	+144	+177	−32	−1	+0.041	−0.010
$_{39}$Y	−10	+103	+106	−11	+9	+0.013	−0.027
$_{40}$Zr	−18	+161	+123	+32	+6	+0.012	+0.056
$_{43}$Tc	+6	−55	−70	+14	+1	−0.006	+0.008
$_{44}$Ru	+8	−49	−75	+22	+4	−0.007	+0.021
$_{48}$Cd	−26	+280	+322	−39	−3	+0.054	−0.005

ulation is small while the *d* charge and its anisotropy is large, as can be seen from the numbers $\Delta n_p, \Delta n_d$ of *p* and *d* electrons deviating from spherical symmetry. Table II shows that the signs of the *p* and *d* contributions, V_{zz}^{pp} and V_{zz}^{dd}, are determined by the signs of the anisotropy counts Δn_p and Δn_d. Thus it is the valence anisotropy which is of prime importance for the EFG, but there is no simple proportionality between V_{zz}^{pp} and Δn_p, V_{zz}^{dd} and Δn_d, respectively. Indeed the radial dependence of the anisotropic charge densities is very important, since in the radial integral in Eq. (3) the $1/r^3$ factor strongly enhances the anisotropic contribution for short distances. Figure 1 shows the radial dependence of the nonspherical charge density $\rho_{20}(r)$, the integrand $\rho_{20}(r)/r^3$ for calculating the valence EFG, and the integral $\int_0^{r'} \rho_{20}(r)/r^3 r^2 dr$ up to a certain r'. While $\rho_{20}(r)$ is largest near the atomic radius, $\rho_{20}(r)/r^3$ has its maximum at short distances from the nucleus. This is the region inside the first node of the *p* wave function which practically determines the EFG. The only exception is Be, where the nodeless 2*p* orbital increases slowly and the contributions from inside the atomic sphere are twice the total EFG.

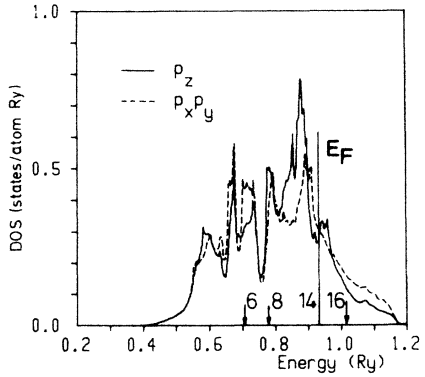

FIG. 3. Decomposition of the partial *p* density of states (DOS) of hcp technecium (in states/atom Ry) into p_z and p_x (p_y) contributions. The arrows indicate the respective Fermi energies for 6 (Y), 8 (Zr), and 16 (Ru) electrons per unit cell.

From the arguments mentioned above it is also clear why the charge density originating from *p* wave functions ("*p* density") dominates over the *d* contribution. The first node of the 5*p* wave function is at much shorter distances than the one of the 4*d* wave function, while the 3*d* wave function is nodeless. In addition, the wave function near the nucleus behaves as r^l, and thus the *d* increases much slower than the *p* density.

In order to show more directly where the nonspherical effects are located, the difference electron densities ($\rho_{\text{solid}} - \rho_{\text{superposed}}^{\text{atom}}$) of Zn are shown in Fig. 2 in the $(11\bar{2}0)$ plane. It is evident, that the superposition of atomic densities generally represents the crystal density quite satisfactorily, but there is a small expansion of the crystal density (i.e., a positive difference density in the interstitial region) and consequently a negative difference density close to the nucleus. It is most important for the EFG that this negative difference density is highly anisotropic, as the clipping in Fig. 2 demonstrates. It is this anisotropy within the clipping which practically completely determines the EFG. The widely used pseudopotential method can be used to easily reproduce the general features of this density, but will not enable us to obtain the (for the EFG) most important anisotropies near the nucleus.

There is another interesting phenomenon, namely the change in sign of the EFG in the 3*d* and 4*d* series, which can be easily understood by inspection of the partial density of states (DOS). In Fig. 3 the p_z and p_x, p_y DOS of

TABLE III. Theoretical valence contributions (without semicore) to the EFG for the 4*d* transition metals: "NE" means number of electrons per unit cell, "true" marks the column with the actual V_{zz}^{val} contribution of that element, "rigid" models these contributions starting from the energy bands of Tc by respective band filling, and E_F is the corresponding Fermi energy (with the Tc bands) in mRy.

Element	NE	True	Rigid	E_F
$_{39}$Y	6	+95	+32	705
$_{40}$Zr	8	+155	+104	777
$_{43}$Tc	14	−56	−56	927
$_{44}$Ru	16	−53	−49	1016

Tc are presented. We notice the dominance of the p_x,p_y DOS at lower energies (up to a band filling of eight electrons), while p_z dominates at higher energies. In a molecular-orbital scheme this DOS can be understood as unsplitted (nonbonding) p_z states and split (bonding and antibonding) p_x,p_y states. Since this DOS does not change much in the $3d$ and $4d$ series a simple band-filling argument leads to more p_x,p_y (Sc, Ti, Y, Zr) or more p_z states (Co, Tc, Ru). Note that all these elements have a rather similar c/a ratio somewhat smaller than the ideal value of 1.633. Table III lists the $4d$ and $5p$ contribution ($V_{zz}^{\rm val}$ without semicore) to the EFG for the $4d$ transition-metal elements. By starting from the energy bands of Tc and using only a rigid band-filling model, we obtain already the correct trend for the sign of the EFG, although the quantitative agreement is as to be expected—fair, but not perfect.

IV. CONCLUSION

We have accurately calculated the EFG's of all hcp metals up to Cd and the results compare favorably with experiment. Our analysis strongly suggests that the EFG is determined by the aspherical electron density distribution of the valence electrons, predominantly from p electrons, close to the nucleus. To obtain this charge distribution reliably both a full-potential and an all-electron calculation is required. The widely used pseudopotential method should not be applied to EFG calculations, and methods based on muffin-tin potentials might yield unreliable results as well.[6]

Some of the more semiempirical methods[5,16,17] attempt to solve the EFG problem from the wrong starting point, i.e., they perform better lattice summations or include additional shielding factors, which are not calculated from first principles for that particular system. We feel that an accurate description of the electronic structure is indispensable. The knowledge of the exact electron density (near the nucleus) is by far the most important part in the calculation of the EFG, and this quantity must be calculated with the highest precision. Thus, even for more complex systems with vacancies, impurities, or surfaces one should not try to explain the EFG with point charges and lattice sums, but with electronic-structure calculations, which can be performed on a highly sophisticated level not only for ordered bulk systems but also for surfaces[18] and impurities.[19] Alternatively, cluster calculations[20,21] may provide sufficient accurate electronic-structure results for nearly all systems, even when they are very complex.

ACKNOWLEDGMENTS

One of us (P.B.) would like to thank the Kernforschungsanlage Jülich for its support during his stay at Jülich.

[1]E. N. Kaufmann and R. J. Vianden, Rev. Mod. Phys. **51**, 161 (1979).
[2]R. Vianden, Hyperfine Interact. **15/16**, 189 (1983).
[3]Th. Wichert and E. Recknagel, *Microscopic Methods in Metals*, in Vol. 40 of *Topics in Current Physics*, edited by U. Gonser (Springer-Verlag, Berlin, 1986).
[4]T. Klas, J. Voigt, W. Keppner, R. Wesche, and G. Schatz, Phys. Rev. Lett. **57**, 1068 (1986).
[5]T. P. Das and P. C. Schmidt, Z. Naturforsch. **41a**, 47 (1986).
[6]P. Blaha, K. Schwarz, and P. Herzig, Phys. Rev. Lett. **54**, 1192 (1985).
[7]P. Blaha and K. Schwarz, Int. J. Quantum Chem. **XXIII**, 1535 (1983).
[8]M. Weinert, J. Math. Phys. **22**, 2433 (1981).
[9]P. Blaha and K. Schwarz, J. Phys. F **17**, 899 (1987). (The present EFG of Be differs in magnitude but not in sign from the value quoted previously, because in the present paper a finer **k** grid and a different exchange-correlation-potential were used and the experimental sign convention is taken.)
[10]J. F. Janak, Solid State Commun. **25**, 53 (1978).
[11]H. R. Kretschmer and J. R. Schneider, Solid State Commun. **49**, 971 (1984).
[12]R. Vianden, Hyperfine Interact. **15/16**, 1081 (1983).
[13]H. Ebert, J. Abart, and J. Voitländer, J. Phys. F **16**, 1287 (1986).
[14]V. R. Green and N. J. Stone, Hyperfine Interact. **30**, 355 (1986).
[15]R. S. Raghavan, E. N. Kaufmann, and P. Raghavan, Phys. Rev. Lett. **34**, 1280 (1975).
[16]E. Bodenstedt, B. Perscheid, and S. Nagel, Z. Phys. B **63**, 9 (1986).
[17]P. C. Pattnaik, M. D. Thompson, and T. P. Das, Phys. Rev. B **16**, 5390 (1977).
[18]E. Wimmer, H. Krakauer, M. Weinert, and A. J. Freeman, Phys. Rev. B **24**, 864 (1981).
[19]P. J. Braspenning, R. Zeller, A. Lodder, and P. H. Dederichs, Phys. Rev. B **29**, 703 (1984).
[20]B. Lindgren, Phys. Rev. B **34**, 648 (1986).
[21]S. Nagel, J. Phys. Chem. Solids **46**, 743 (1985).

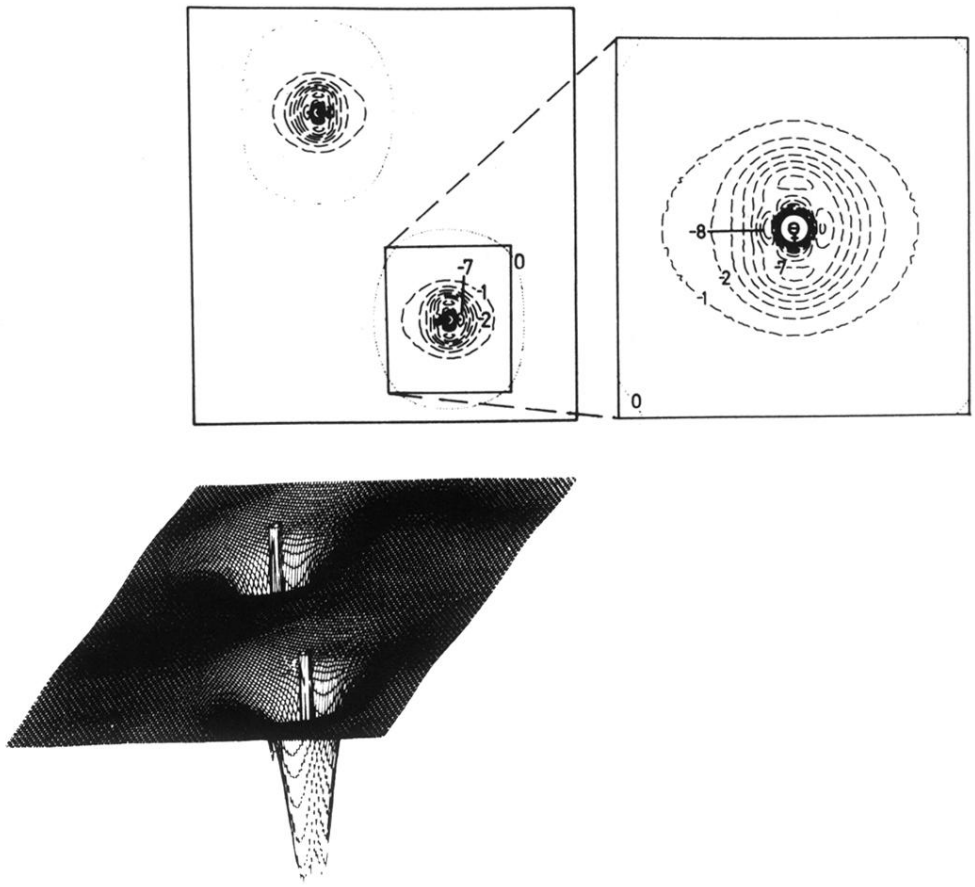

FIG. 2. Difference electron densities of hcp Zn in the $(11\bar{2}0)$ plane. The cutoff of the perspective plot is 0.08 e/a.u.^{3} In the contour plot units of me/a.u.^{3} are used.